

Study of the fission path energy of U-236 using microscopic mean-field model

Kazuki FUJIO^{†1}, Shuichiro EBATA², Tsunenori INAKURA¹, and Satoshi CHIBA¹

¹*Tokyo Institute of Technology, Ookayama2-12-1, Meguro, Tokyo, 152-8850, Japan*

²*Saitama University, Shimo-Okubo255, Sakura-ku, Saitama, 338-8570, Japan*

[†]*E-mail: fujio.k.aa@m.titech.ac.jp*

Abstract

To study a fission path, we investigated the potential energy surface of U-236 with respect to its quadrupole and octupole deformations, using the microscopic theoretical model with Skyrme-type effective interactions. We divided the potential energy surface into 7 terms to investigate their contributions to the fission barrier height. Although the height is decided from the competition among the terms, we found the Coulomb term and a combination of others excluding the spin-orbit and pairing energy terms have a relatively small interaction dependence. It indicates that the amplitudes of spin-orbit and pairing energy will affect the barrier height.

1 Introduction

Minor Actinides (MA) are produced through a sequence of neutron-capture, β -, and α -decays in nuclear reactors. The MAs affect the performance of nuclear reactors and the composition of nuclei in the radioactive waste. Therefore, nuclear data such as the fission product yield of MA is necessary for reactor technology and to deal with the radioactive waste effectively. However, the data is insufficient and its uncertainty is large, due to the difficulty of experiments using highly radioactive materials. A theoretical approach is one of the effective techniques to prepare unmeasured data or to predict unmeasurable data. The macro-micro models [1, 2] that consist of the liquid drop model [3] and a quantum correction have been employed widely for the fission study. The liquid drop model is employed to describe the bulk property of the nucleus, and the quantum correction is introduced for the nuclear shell effects. The parameters in the model and correction are phenomenologically determined to reproduce the nuclear properties well. Although the model works well to explain and reproduce the known data, its prediction power might be small for unknown data. To supply and predict the data of MA or unmeasured, we should have a more fundamental approach in which the empirical methods are excluded as far as possible. Therefore we employ a microscopic mean-field model that can describe nuclei from the degree of freedom of nucleon to investigate the fission phenomena. Our model employs the Skyrme effective interaction [4], which has been developed to describe the basic nuclear properties in the vicinity of ground states: nuclear binding energy, nuclear matter parameters, radius, deformation, and shell structure. We should investigate carefully the applicability of these effective interactions to be applied to nuclear fission because the nuclei become much deformed in the way to scission hence they are far from their ground states. In this study, we calculate the potential energy surface (PES) of the U-236 assuming the compound nucleus of $n + \text{U-235}$ reaction, and investigate the difference among the PES given by existing Skyrme effective interactions.

2 Method

We employ the Skyrme-Hartree-Fock+BCS model [5] and impose constraints on the nuclear shape [6] of U-236. To describe any nuclear deformation in this work, the wave function is represented in the three-dimensional coordinate space. The three Skyrme effective interactions (SkM*, SLy4, SkI3) are employed. The Skyrme effective interaction is written with the delta function of a space r , as follows:

$$\begin{aligned} \hat{v}(i, j) = & t_0(1 + x_0 P_\sigma) \delta(\mathbf{r}) + \frac{1}{2} t_1(1 + x_1 P_\sigma) \left(\mathbf{k}^2 \delta(\mathbf{r}) + \delta(\mathbf{r}) \mathbf{k}'^2 \right) + t_2(1 + x_2 P_\sigma) \mathbf{k} \cdot \delta(\mathbf{r}) \mathbf{k}' \\ & + \frac{1}{6} t_3(1 + x_3 P_\sigma) \rho^\alpha \left(\frac{\mathbf{r}_i + \mathbf{r}_j}{2} \right) \delta(\mathbf{r}) + iW(\boldsymbol{\sigma}_i + \boldsymbol{\sigma}_j) \cdot \mathbf{k} \times \delta(\mathbf{r}) \mathbf{k}', \end{aligned} \quad (1)$$

where $t_0, x_0, t_1, x_1, t_2, x_2, t_3, x_3, \alpha, W$ are parameters, $\boldsymbol{\sigma}$ is the Pauli matrix, P_σ is the spin exchange operator, \mathbf{k} and \mathbf{k}' are relative momenta. The \mathbf{k} (\mathbf{k}') is formed $(\vec{\nabla}_i - \vec{\nabla}_j)/2i$ ($(\vec{\nabla}_i - \vec{\nabla}_j)/2i$) which acts on the right (left) side. These parameters are adjusted to reproduce nuclear properties according to the protocol of each parameter set. The SkM* parameter set is to reproduce the fission barrier height of the Pu-240 [7], the SLy4 is designed to deduce the nucleon matter properties [8], and the SkI3 is prepared to reproduce the single-particle states of Pb-208 which the relativistic mean-field model deduces [9]. We can calculate the energy of a system from the expectation value of the Skyrme interaction by the many-body wave function. Normally, Skyrme interaction is divided into the central force and spin-orbit force. However, it is divided into the four forces because we want to investigate the behavior of each term in detail. The first term in Eq.(1) is named volume term which works as the attractive force, the second and third terms are reflected the nuclear surface properties due to including the differential operators. The fourth term is named density-dependent term which works as a repulsive force. The last term means the spin-orbit force. The many-body wave function formed as BCS-type [10] is employed in which the single-particle states and the pairing correlation are determined self-consistently. We calculate the PES of U-236 in which the fission reaction of U-235 induced a thermal neutron is assumed. The constraints on nuclear shape are expressed with the radial direction r and the spherical harmonics Y_{lm} . The quadrupole \hat{Q}_{20} and octupole \hat{Q}_{30} operators are applied to express the elongation and mass asymmetry of the nucleus, respectively. Their forms are:

$$\begin{aligned} \hat{Q}_{20} &= r^2 Y_{20} = \sqrt{\frac{5}{16\pi}} r^2 (3 \cos^2 \theta - 1), \\ \hat{Q}_{30} &= r^3 Y_{30} = \sqrt{\frac{7}{16\pi}} r^3 (5 \cos^3 \theta - 3 \cos \theta). \end{aligned} \quad (2)$$

For the investigation of the fission path, the PES is calculated with these constraints. The constraints are introduced to the Hamiltonian \hat{H} , such as Lagrange multiplier:

$$\hat{H}' = \hat{H} - \sum_{l=2,3} \lambda_{l0} \left(\hat{Q}_{l0} - Q_{l0} \right)^2, \quad (3)$$

where λ_{l0} is the Lagrange multiplier and Q_{l0} is the expectation value $\langle \hat{Q}_{l0} \rangle$ with the many-body wave function. The procedure to calculate the PES is 1) to prepare the ground state, 2) to elongate the nucleus with using \hat{Q}_{20} , and 3) to add the octupole moment using \hat{Q}_{30} for the expression of mass asymmetry.

3 Results and discussion

Figure 1 shows the PES with respect to Q_{20} and Q_{30} using SkI3 parameter set. The PES dE can be calculated as the difference between the ground state energy $E_{G.S.}$ and the energy at the

each point $E(Q_{20}, Q_{30})$, and as follows;

$$dE = E(Q_{20}, Q_{30}) - E_{G.S.} \quad (4)$$

The dashed line shows the symmetry fission path corresponding to $Q_{30} = 0$, and the solid line shows a path following a valley of the PES in Figure 1. Nucleon densities at some important points are given in this figure, additionally, it is clear that the path written by the solid line is easier to undergo fission than the dashed one. Figure 2 shows the results of dE along the two fission paths. The dashed and the solid line are the same as in Figure 1. All of interactions have the ground state, the 2nd minimum, the inner fission barrier B_{inner} and the outer fission barrier B_{outer} . The two-humped barrier structure can be seen for the three effective interactions and the mass asymmetric deformation allows the decreasing the B_{outer} . Our results and the experimental data for $E_{G.S.}$ [12] and for the fission barrier heights are shown in Table 1.

Table 1: Calculation results for $E_{G.S.}$, B_{inner} , $B_{\text{outer}}(Q_{30} = 0)$ and $B_{\text{outer}}(Q_{30} \neq 0)$ using different Skyrme interactions together with experimental values

Force	SkM*	SLy4	SkI3	exp.
$E_{G.S.}$ (MeV)	-1796.97	-1796.46	-1799.85	-1790.41
B_{inner} (MeV)	8.4	10.4	8.7	4.9
$B_{\text{outer}}(Q_{30} = 0)$ (MeV)	13.1	18.1	14.2	-
$B_{\text{outer}}(Q_{30} \neq 0)$ (MeV)	7.2	10.2	6.3	5.8

This result reveals that our calculation overestimates the experimental data of the fission barrier height [11]. To elucidate the reason for this overestimation, we investigate which terms contribute to and which manner to the fission barrier in the following.

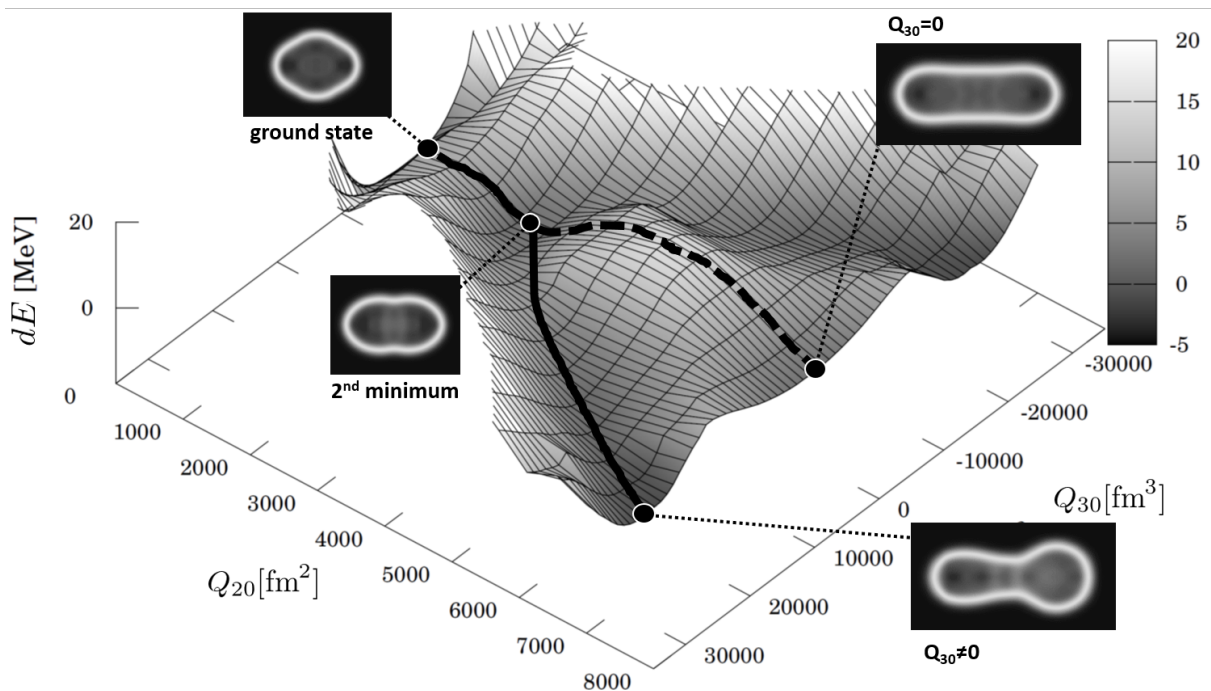


Figure 1: The PES of SkI3 with respect to Q_{20} and Q_{30}

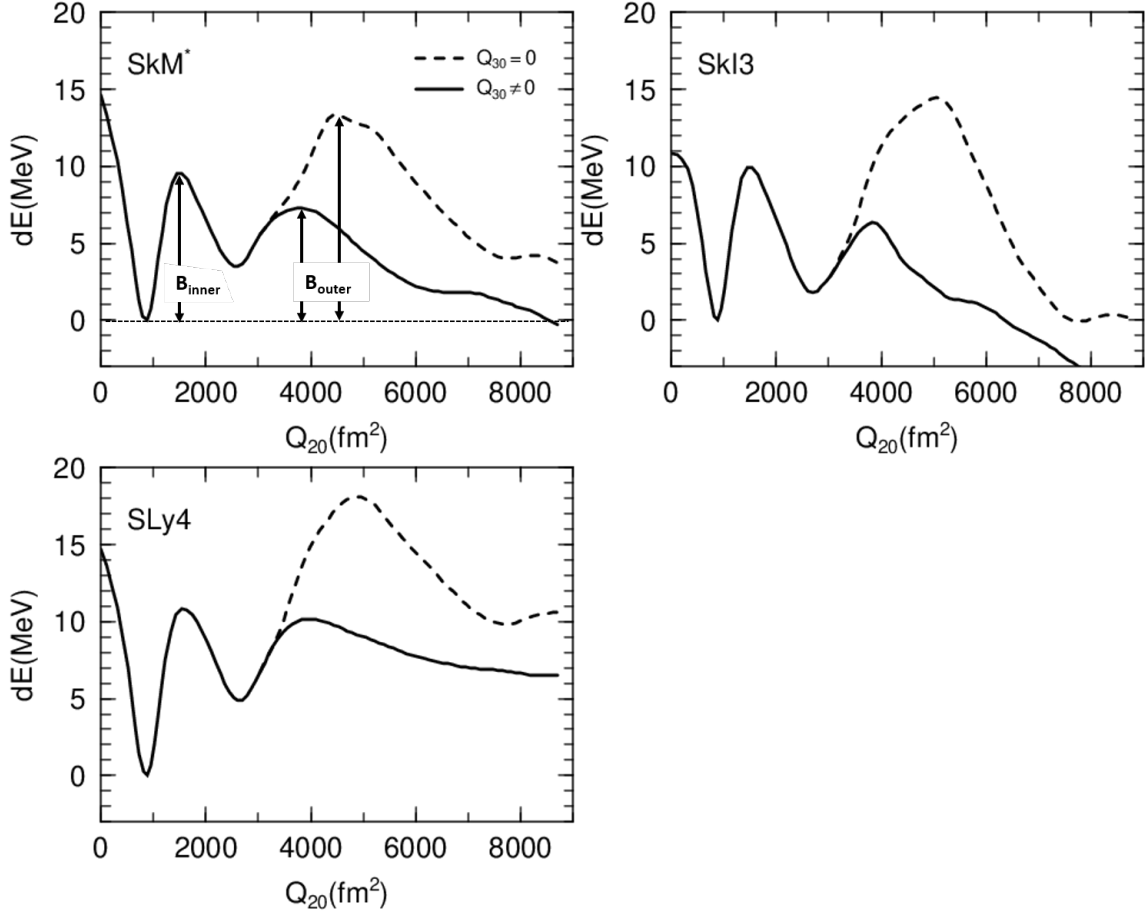


Figure 2: The fission path with respect to Q_{20}

The total binding energy E_{tot} of each interaction can be divided into 7 terms which are E_{t0} , $E_{t1,t2}$, E_{t3} , E_{ls} , the kinetic energy $E_{kinetic}$, the Coulomb energy $E_{Coulomb}$, and the pairing energy E_{pair} :

$$\begin{aligned}
 E_{tot} &= E_{t0} + E_{t1,t2} + E_{t3} + E_{ls} + E_{kinetic} + E_{Coulomb} + E_{pair} \\
 &= E_{Skyrme} + E_{kinetic} + E_{Coulomb} + E_{pair}.
 \end{aligned} \tag{5}$$

The Skyrme energy E_{Skyrme} is composed of the volume energy E_{t0} , the surface energy $E_{t1,t2}$, the density dependence energy E_{t3} , and the spin-orbit energy E_{ls} . It is difficult to specify their contributions to the fission barrier because they have a complicated competition. To extract the major characterizing the barrier, we search a combination of the energy terms which have a small interaction-dependence, namely, the non-characteristic parts of the PES on all interactions.

Figure 3 shows the result of them. These energies is calculated as the same way of Eq.(4). The solid line shows SkM*, the dashed one is SLy4 and the dotted one is SkI3. The left panel represents the sum of $E_{t0} + E_{t1,t2} + E_{t3} + E_{kinetic}$. This summation increases with increasing Q_{20} for the three effective interactions. On the other hand, $E_{Coulomb}$ decreases with increasing Q_{20} , because the Coulomb force is inversely proportional to the distance of the charge. There are small interaction dependences on the sum of $E_{t0} + E_{t1,t2} + E_{t3} + E_{kinetic}$ and $E_{Coulomb}$, which indicates that the E_{ls} and E_{pair} have a very important role to form the fission barrier.

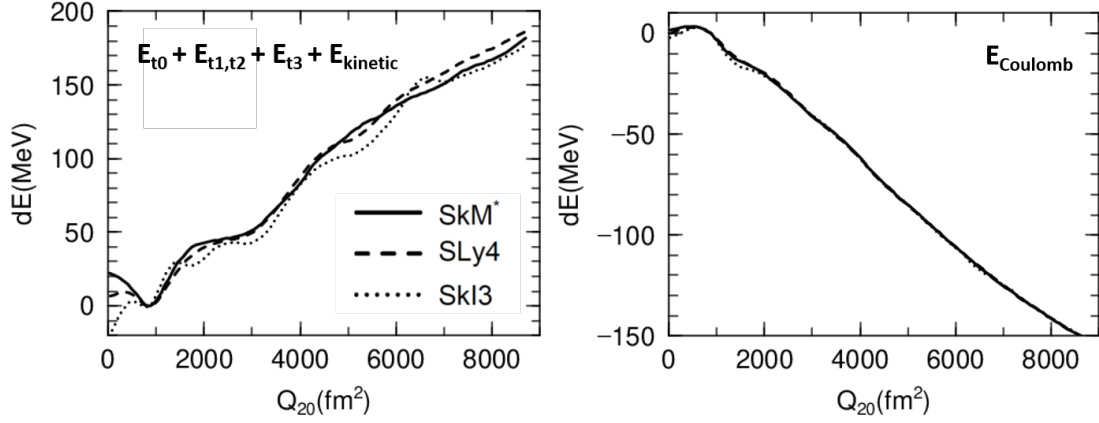


Figure 3: The contributions for dE : (left) $E_{t0} + E_{t1,t2} + E_{t3} + E_{kinetic}$, and (right) $E_{Coulomb}$

The behavior of the E_{ls} and E_{pair} are compared with the fission path in Figure 4. The upper left (right) shows E_{ls} (E_{pair}) and the lower left shows the fission path. The solid (dotted) arrow indicates a bump (valley) of the fission path. These results show that E_{ls} has in-phase and, E_{pair} has the out-of-phase with the fission path. The phase relationship between the spin-orbit force and the pairing correlation has been known for the previous nuclear structure study [13]. We point out that there are small interaction dependences on the sum of $E_{t0} + E_{t1,t2} + E_{t3} + E_{kinetic}$ and $E_{Coulomb}$. Therefore, the E_{ls} and E_{pair} might have an important role to decide the fission barrier height.

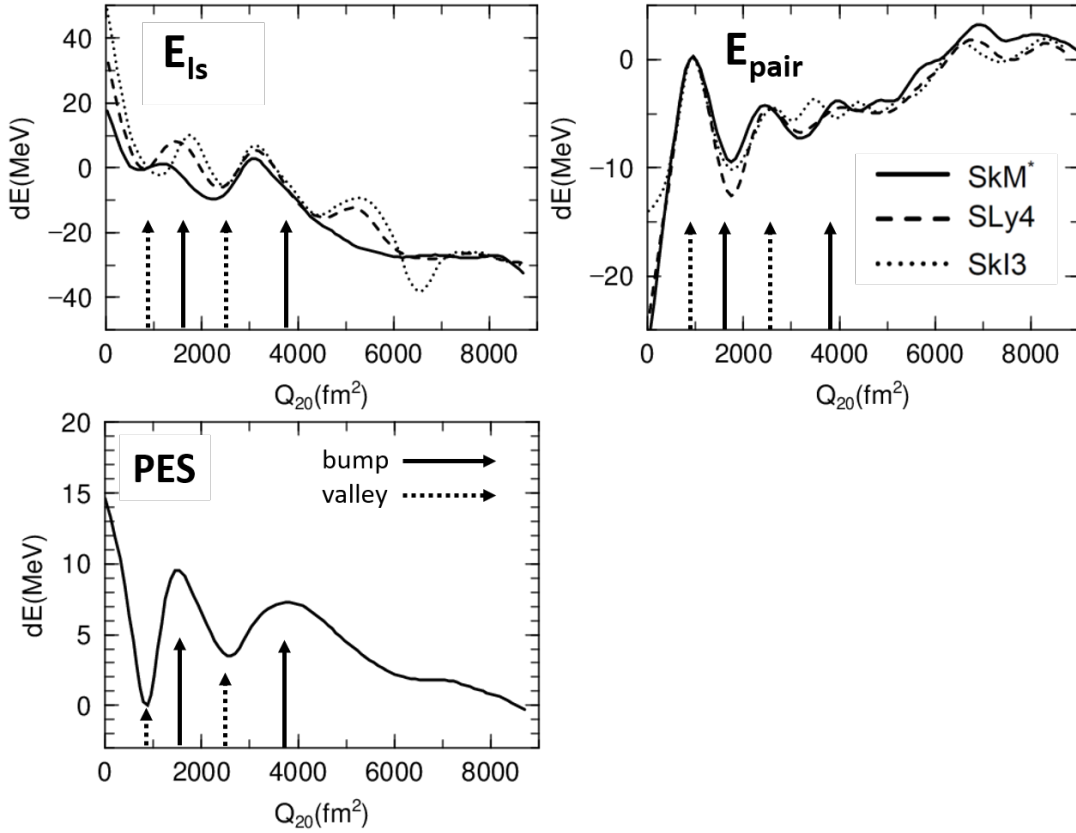


Figure 4: The behavior of the E_{ls} and E_{pair}

4 Conclusion

We investigate the PES of U-236 by the constraint Skyrme-Hartree-Fock+BCS with respect to the quadrupole Q_{20} and octupole Q_{30} momentums. Our calculation reproduces the two-humped barrier structure on the fission path, shows also that the degree of freedom for the mass asymmetry on fission products, namely, Q_{30} effects, allows the decreasing the outer barrier height. The calculated fission barriers overestimate the experimental data. In order to elucidate the reason for the overestimation, the fission path is decomposed into 7 terms. The sum of $E_{t0} + E_{t1,t2} + E_{t3} + E_{\text{kinetic}}$, and the E_{Coulomb} have a small interaction-dependence. Thus, the E_{ls} and E_{pair} might affect the fission barrier height.

Acknowledgement

This work is supported by the Leading initiative for Excellent Young Researchers, MEXT, Japan, and by the Japan Society for the Promotion of Science (JSPS) KAKENHI Grant Number JP20K03943.

References

- [1] V. M. Strutinsky, Shell effects in nuclear masses and deformation energies, Nucl. Phys. **A95**, 1967, pp.420–442.
- [2] V. M. Strutinsky, “Shells” in deformed nuclei, Nucl. Phys. **A122**, 1968, pp.1–33.
- [3] N. Bohr and J. A. Wheeler, The Mechanism of Nuclear Fission, Phys. Rev. **56**, 1939, pp.426–450.
- [4] D. Vautherin and D. M. Brink, Hartree-Fock Calculations with Skyrme’s Interaction. I. Spherical Nuclei, Phys. Rev. **C5**, 1972, pp.626–647.
- [5] S. Ebata and T. Nakatsukasa, Octupole deformation in the nuclear chart based on the 3D Skyrme Hartree–Fock plus BCS model, Phy. Scr. **92**, 2017 pp.064005
- [6] G. Scamps and C. Simenel, Impact of pear-shaped fission fragments on mass-asymmetric fission in actinides, Nature. **564**, 2018, pp.382–385.
- [7] J. Barrel et al., Towards a better parametrisation of Skyrme-like effective forces: A critical study of the SkM force, Nucl. Phys. **A386**, 1982, pp.79–100.
- [8] E. Chabanat et al., A Skyrme parametrization from subnuclear to neutron star densities Part II. Nuclei far from stabilities, Nucl. Phys. **A635**, 1998, pp.231–256.
- [9] P.-G. Reinhard and H. Flocard, Nuclear effective forces and isotope shifts, Nucl. Phys. **A584**, 1995, pp.467–488.
- [10] Bardeen et al., Theory of Superconductivity, Phys. Rev. **108**, 1957, pp.1175–1204.
- [11] T. Belgya et al., Handbook for Calculations of Nuclear Reaction Data RIPL-2,IAEA = TECDOC-1506., 2006.
- [12] AMDC-Atomic Mass Data Center -IAEA-NDS
<https://www-nds.iaea.org/amdc/>
- [13] S. G. Nilsson and I. Ragnarsson, SHAPES AND SHELLS IN NUCLEAR STRUCTURE, CAMBRIDGE UNIVERSITY PRESS, 1995.